0273-2289/97/620203—0275$12.00

Antigen-Antibody Binding Kinetics for Biosensor Applications

A Dual-Fractal Analysis

AJIT SADANA* AND MILIND SUTURIA

Chemical Engineering Department, University of Mississippi, University, MS 38677-9740

Received January 22, 1996; Accepted March 14, 1996

ABSTRACT

The diffusion-limited binding kinetics of antigen (or antibody) in solution to antibody (or antigen) immobilized on a biosensor surface is analyzed within a fractal framework. The fit obtained by a dual-fractal analysis is compared with that obtained from a single-fractal analysis. In some cases, the dual-fractal analysis provides an improved fit when compared with a single-fractal analysis. This was indicated by the regression analysis provided by Sigmaplot (San Rafael, CA). These examples are presented. It is of interest to note that the state of disorder (or the fractal dimension) and the binding rate coefficient both increase (or decrease, a single example is presented for this case) as the reaction progresses on the biosensor surface. For example, for the binding of monoclonal antibody MAb 49 in solution to surface-immobilized antigen, a 90.4% increase in the fractal dimension (D_{f1} to D_{f2}) from 1.327 to 2.527 leads to an increase in the binding rate coefficient (k_1 to k_2) by a factor of 9.4 from 11.74 to 110.3. The different examples analyzed and presented together provide a means by which the antigen-antibody reactions may be better controlled by noting the magnitude of the changes in the fractal dimension and in the binding rate coefficient as the reaction progresses on the biosensor surface.

Index Entries: Antigen-antibody binding kinetics; fractals; biosensors.

INTRODUCTION

Sensitive detection systems (or sensors) are required to distinguish a wide range of substances. Sensors find application in the areas of biotech-

*Author to whom all correspondence and reprint request should be addressed.
E-mail: cmsadana@olemiss.edu.

nology, physics, chemistry, medicine, aviation, and environmental control. Biosensors have different operating parameters such as stability, specificity, response time, selectivity, regenerability, etc. A better understanding of the mode of operation of these parameters would lead to increasing biosensor performance efficiency. The solid-phase immunoassay technique represents a convenient method for the separation and/or detection of reactants (for example, antigen) in a solution. The binding of the antigen to an antibody-coated surface (or vice-versa) is sensed directly and rapidly. There is a need to characterize the reactions occurring at the biosensor surface.

Pisarchick et al. *(1)* have indicated that the details of the association of antibodies (or antigens) with the antigen-coated (or antibody-coated) surfaces are of tremendous significance for the development and characterization of immunodiagnostic devices, as well as for biosensors. McLean et al. *(2)* indicate the importance of selectively controlling molecular recognition events at a protein-substrate (or in our case antibody-antigen) interface. McLean et al. *(2)* emphasize that controlling the orientation of immobilized proteins (or in the general case, "receptors") is a straightforward method for controlling the reactions at the interface.

Maxia et al. *(3)* have recently characterized Langmuir-Blodgett films of rhodopsin. These authors indicate that the Langmuir-Blodgett (L-B) technique has expanding applications in molecular electronic devices and in biosensors. This technique permits the production of thin films or dense monolayers of ordered structures such as the antigens or antibodies on a biosensor surface. This ordered structure on the biosensor surface minimizes (or makes negligible) the binding irregularities of antigen to antibody. Dubrovsky et al. *(4)* have recently analyzed the immunological activity of IgG L-B monolayers organized with the assistance of a protein A sublayer. These authors compared their results using a protein A sublayer with direct deposition of the IgG monolayer on the surface. Using the protein A sublayer to orient the IgG molecules, Dubrovsky et al. *(4)* not only obtained a higher specific sensitivity for the IgG film, but also the nonspecific binding was lower. Ordered structures on the surface and decreases in the nonspecific binding would help control the reactions at the surface, besides minimizing the heterogeneity at the biosensor surface.

External diffusional limitations play a role in immunoassays *(5–7)*. The influence of diffusion in such systems has been analyzed to some extent *(8–14)*. There are limitations to classical modeling techniques that do not account for heterogeneity at the reaction surface. Douglas *(15)* emphasizes that naturally occurring surfaces (cell membranes and organelles, soils, colloidal aggregates, and so on) tend to be highly irregular and need to be characterized appropriately. It is to be reasonably anticipated that the immobilization procedure utilized to attach the antigen or antibody to the biosensor surface would yield an "irregular surface."

Ortega-Vinuesa et al. *(16)* have recently compared the immunological efficiencies of a physically adsorbed and chemically bound IgG to carboxy-

lated latexes (CLs). These authors emphasize that CLs are excellent carriers of antibodies or antigens since they possess a chemical group to which the antibody or the antigen may be attached. These authors noted that the chemically bound IgG to CLs have several distinct advantages in that there is no decrease in the immunological activity (since denaturation is prevented), no desorption of antibodies, minimal non-specific adsorption or binding, and uniform coupling is obtained. All of these factors in the chemical binding procedure lead to a decrease in the heterogeneity on the surface.

Kopelman *(17)* indicates that surface diffusion-controlled reactions that occur on clusters or islands are expected to exhibit anomalous and fractal-like kinetics. These fractal kinetics exhibit anomalous reaction orders and time-dependent rate (i.e., binding) coefficients. Fractal kinetics have been observed in diffusion-controlled reactions in disordered materials *(18,19)*. Werthen and Nygren *(20)* have emphasized the difference in the reaction mechanism for the antibody binding to surface-immobilized antigen (or vice-versa), and for antibody-hapten reactions in solution. Often, the association (binding) rate coefficient decreases continuously with time. Fractals are disordered systems, and the disorder is described by nonintegral dimensions *(21)*. These authors further indicate that as long as surface irregularities show scale invariance that is dilatational symmetry, they can be characterized by a single number, the fractal dimension.

Antibodies are heterogeneous and their immobilization on a fiberoptic surface, for example, would result in some degree of heterogeneity. This is a good example of a "disordered system" for which a fractal analysis is appropriate. In this type of diffusion-reaction system, the diffusion is conventional in the sense that it follows the classical diffusion equation: It is the boundary condition on the fractal surface (biosensor surface, in our case) that is more complex. Moreover, the antigen-antibody reaction on the surface is a typical low-dimension reaction system, in which the distribution tends to be "less random" *(17)*. Fractal analyses using a single fractal dimension have provided physical clarification of the diffusion-controlled reactions at the surface *(14,22–27)*. It was noted in the aforementioned analyses that for some biosensor applications there was room for improvement in the "single-fractal" dimension analysis as far as fitting the data was concerned. More refined fits may be obtained if a multi-fractal analysis instead of a single-fractal analysis is used to model some selected data.

Skinner *(28)* emphasizes that for chaos in biological systems only a few variables govern the spatial and temporal geometries of the system. An understanding of these fractal attractors or dimensions will significantly assist in the control of these complex systems. Cross and Hohenberg *(29)* have recently indicated that some systems that display spatiotemporal chaos are said to be large since their description requires (more than one) a number of chaotic elements or attractors distributed in space. Multifractal analysis has also been indicated in adsorption *(30)*. Friesen and Laidlaw *(31)* when analyzing coal samples indicate the possibility of the existence of two fractal dimen-

sions that characterize a system or surface, and caution against "well fitting" the data (albeit incorrectly) by a single line or fractal dimension. Extreme care must be utilized to fit data, especially at the lower fractal dimensions. Glockle and Nonnenmacher *(32)* recently indicate that scaling laws and self-similar behavior are a characteristic of complex systems. Shlesinger et al. *(33)* emphasize that in anomalous transport systems kinetic averaging leads to scaling laws and multifractal properties. Scaling behavior has also been observed for a theoretical analysis of two-dimensional diffusive dynamics *(34)*.

A dual-fractal analysis is presented for the kinetics of the binding of the antigen (or antibody) in solution to antibody (or antigen) immobilized on the biosensor surface. The experimental data is carefully screened; only that data is used wherein a dual-fractal analysis provides a significant improvement in the fit compared to a single-fractal analysis. Often, a single fractal dimension analysis provides a reasonable fit. This data was not used in the present analysis. Furthermore, for the examples analyzed, both the single- and the dual-fractal analysis is presented. This clearly delineates the necessity of the dual-fractal analysis vis-à-vis the single-fractal analysis.

THEORY

An analysis of the binding kinetics of antigen in solution to antibody immobilized on the biosensor surface is available *(11,12)*. The influence of lateral interactions on the surface and variable rate coefficients is also available *(13)*. Here we present a method of estimating actual fractal dimension values for antibody-antigen binding systems utilized in fiberoptic biosensors.

VARIABLE BINDING RATE COEFFICIENT

Kopelman *(17)* has recently indicated that classical reaction kinetics is sometimes unsatisfactory when the reactants are spatially constrained on the microscopic level by either walls, phase boundaries, or force fields. Such heterogeneous reactions, for example, bioenzymatic reactions, that occur at interfaces of different phases exhibit fractal orders for elementary reactions and rate coefficients with temporal memories. In such reactions, the rate coefficient exhibits a form given by:

$$k_1 = k' t^{-b} \quad 0 < b < 1 \quad (t = 1) \tag{1}$$

In general, k_1 depends on time, whereas $k' = k_1$ $(t = 1)$ does not. Kopelman *(17)* indicates that in three dimensions (homogeneous space), $b = 0$. This is in agreement with the results obtained in classical kinetics. Also, with vigorous stirring, the system is made homogeneous and $b = 0$. However, for diffusion-limited reactions occurring in fractal spaces, $b > 0$; this yields a time-dependent binding rate coefficient.

The random fluctuations on a two-state process in ligand binding kinetics has been analyzed *(35)*. The stochastic approach can be used as a

means to explain the variable binding rate coefficient. The simplest way to model these fluctuations is to assume that the binding rate coefficient k_1 *(t)* is the sum of its deterministic value (invariant) and the fluctuation [z(t)] *(35)*. This *z(t)* is a random function with a zero mean. The decreasing and increasing binding rate coefficients can be assumed to exhibit an exponential form *(11,13,36)*:

$$k_1 = k_{1,0} \exp(-\beta t)$$
$$k_1 = k_{1,0} \exp(\beta t) \tag{2}$$

Here, β and $k_{1,0}$ are constants.

Sadana and Madagula *(13)* have analyzed the influence of a decreasing and an increasing binding rate coefficient on the antigen concentration near the surface when the antibody is immobilized on the surface. These authors noted that for an increasing binding rate coefficient, after a brief time interval, as time increases, the concentration of the antigen near the surface decreases, as expected for the cases when lateral interactions are present or absent. The diffusion-limited binding kinetics of antigen (or antibody or substrate) in solution to antibody (or antigen or enzyme) immobilized on a biosensor surface has been analyzed within a fractal framework *(22,27)*. Furthermore, experimental data presented for the binding of HIV virus (antigen) to the antibody anti-HIV immobilized on a surface displays a characteristic ordered "disorder" *(37)*. This indicates the possibility of a fractal-like surface. It is obvious that the aforementioned biosensor system (wherein either the antigen or the antibody is attached to the surface) along with its different complexities that include heterogeneities on the surface and in solution, diffusion-coupled reaction, time-varying adsorption or binding rate coefficients, and so on, can be characterized as a fractal system.

The diffusion of reactants toward fractal surfaces has been analyzed *(38–41)*. Havlin *(42)* has briefly reviewed and discussed the results. Sadana and Madagula *(26)* have recently presented a theoretical analysis using fractals for the time-dependent binding of antigen in solution to antibody immobilized on a fiberoptic biosensor surface. The authors noted that an increase in the fractal dimension utilized in their studies decreased both the rate of antigen binding and the amount of antigen bound.

Single-Fractal Analysis

Havlin *(42)* indicates that the diffusion of a particle [antibody (Ab)] from a homogeneous solution to a solid surface [antigen (Ag)-coated biosensor surface] where it reacts to form a product (antibody-antigen complex; Ab.Ag) is given by:

$$(\text{Ab.Ag}) \sim \begin{cases} t^{(3-D_f)/2} = t^p & t < t_c \\ t^{1/2} & t > t_c \end{cases} \tag{3}$$

Here, D_f is the fractal dimension of the surface. Equation (3) indicates that the concentration of the product Ab.Ag (t) in a reaction Ab + Ag → Ab.Ag on a solid fractal surface scales at short and intermediate scales as Ab.Ag $(t) \sim t^p$ with the coefficient $p = (3 - D_f)/2$ at short time scales, and $p = 1/2$ at intermediate time scales. This equation is associated to the short-term diffusional properties of a random walk on a fractal surface. Note that in a perfectly stirred kinetics on a regular (nonfractal) structure (or surface), k_1 is a constant, that is, it is independent of time. In other words, the limit of regular structures (or surfaces) and the absence of diffusion-limited kinetics leads to k_1 being independent of time. In all other situations one would expect a scaling behavior given by $k_1 \sim k' t^{-b}$ with $-b = p < 0$. Also, the appearance of the coefficient, p different from $p = 0$ is the consequence of two different phenomena, that is heterogeneity (fractality) of the surface, and the imperfect mixing (diffusion-limited condition).

Havlin *(42)* indicates that the crossover value may be determined by $r^2_c \sim t_c$. Above the characteristic length, r_c, the self-similarity of the surface is lost. Above t_c, the surface may be considered homogeneous, since the self-similarity property disappears and "regular" diffusion is now present. For the present analysis, t_c is arbitrarily chosen. One may consider the analysis to be presented as an intermediate heuristic approach in that in the future one may also be able to develop an autonomous (and not time-dependent) model of diffusion-controlled kinetics in disordered media.

Dual-Fractal Analysis

The single-fractal analysis presented above is extended to include two fractal dimensions. At present, the time ($t = t_1$) at which the first fractal dimension changes to the second fractal dimension is arbitrary and empirical. For the most part it is dictated by the data analyzed and experience gained by handling a single-fractal analysis. In this case, the product (antibody-antigen complex, Ab.Ag) concentration on the biosensor surface is given by:

$$(\text{Ab.Ag}) \sim \begin{cases} t^{(3-D_{f1})/2} = t^{p_1} & t < t_1 \\ t^{(3-D_{f2})/2} = t^{p_2} & t_1 < t < t_2 = t_c \\ t^{1/2} & t > t_c \end{cases} \qquad (4)$$

RESULTS

A Comparision of a Dual-Fractal Analysis with a Single-Fractal Analysis

Initially, the fit obtained by a dual-fractal analysis is compared to that obtained from a single-fractal analysis for selected cases of antigen-antibody binding for biosensor applications.

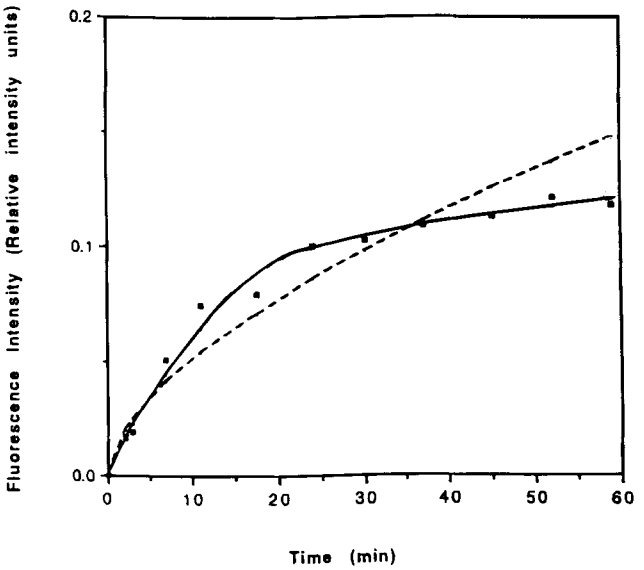

Fig. 1. Theoretical curves using Eq. (3) (——) and Eq. (4) (____) for the binding of FITC-avidin in solution to sensor tips doped with 0.28 mole% B-DPPE (original data from Zhao and Reichert, 1992).

Zhao and Reichert (42) analyzed the time-dependent fluorescence intensity of the binding of FITC-avidin in solution to sensor tips doped with 0.28 mol% B-DPPE. Fig. 1 shows the curves obtained using Eq. 2 and 4 for the binding of FITC-avidin. Table 1 shows the values of the binding rate coefficient, k and the fractal dimension, D_f using a single-fractal analysis (Eq. 3), a biphasic function of time, and the values of the binding rate coefficients, k_1 and k_2, and the fractal dimension values, D_{f1} and D_{f2} using a dual-fractal analysis (Eq. 4), a triphasic function of time, to model the experimental data. The parameter values presented in Table 1 were obtained from a regresssion analysis using Sigmaplot (San Raphael, CA) to model the experimental data using eqs. 3 and 4, wherein (Ab.Ag) = kt^p (single-fractal analysis), and (Ab.Ag) = $kt^{(p_1 \text{ or } p_2)}$ (dual-fractal analysis). The k, D_f, k_1, k_2, D_{f1}, and D_{f2} values presented in Table 1 are within 95% confidence limits. For example, the value of k reported for B-DPPE in Table 1 is 0.13 ± 0.003. The 95% confidence limits indicates that 95% of the k values will fall between 0.133 and 0.127. This indicates that the values are precise and significant. The Sigmaplot program provided the values of k and p (single-fractal analysis), and k_1, k_2, p_1, and p_2 (dual-fractal analysis). The values of p, p_1, and p_2 are not given. To conserve space, only the values of D_f, D_{f1}, and D_{f2} are given. The curves presented in Fig. 1 are theoretical curves. Figure 1 clearly shows that the dual-fractal analysis provides a better fit than that provided by a single-fractal analysis, and thus the necessity of the dual-fractal analysis vis-á-vis the single-fractal analysis.

Table 1
Fractal Dimensions and Binding Rate
Coefficients for Different Antigen-Antibody Binding Reactions

Antibody Concentration	k	D_f	k_1	k_2	D_{f1}	D_{f2}	Ref.
B-DPPE	0.13 ±0.003	1.81 0.11	0.01 ±0.002	0.05 ±0.001	1.37 ±0.19	2.57 0.05	42
Mab 49	23.1 ±3.41	1.79 ±0.07	11.7 ±0.28	110 ±1.67	1.33 ±0.02	2.53 ±0.02	43
Mab 53	4.46 ±0.93	1.05 ±0.06	2.38 ±0.21	17.8 ±0.99	0.52 ±0.06	1.74 ±0.05	43
Mab 57	24.7 ±3.47	1.61 ±0.05	15.9 ±0.66	76.7 ±1.06	1.24 ±0.05	2.17 ±0.02	43
30 µg/mL Mab 53	6.57 ±0.76	1.73 ±0.51	4.94 ±0.40	41.4 ±0.32	1.06 ±0.06	2.11 ±0.03	43
100 µg/mL Mab 53	27.3 ±6.3	1.22 ±0.47	9.09 ±0.65	97.3 ±3.5	0.863 ±0.079	2.40 ±0.03	43
25 µL of antibody (12 ng; 5×10^4 cpm) and 25 µL of 0.5% deoxycholate	26.9 ±4.03	2.77 ±0.07	14.3 ±0.50	40.8 ±0.15	1.98 ±0.09	2.99 ±0.001	44
25 µL of antibody was preincubated for 60 min with 25 µl of brain Thy-1 antigen (12.5 ng) in 0.5% deoxycholate	3.72 ±0.29	2.05 ±0.07	2.66 ±0.12	6.67 ±0.07	1.83 ±0.08	2.33 ±0.04	44
25 µL of ^{125}I-labeled rabbit F(ab′)$_2$ anti-Thy-1 antibody in 0.5% deoxycholate	3.77 ±0.19	2.54 ±0.06	2.84 ±0.08	5.25 ±0.05	2.34 ±0.05	2.70 ±0.05	44
anti-BPT (regenerable biosensor)	38.7 ±5.49	1.96 ±0.09	52.2 0.80	6.75 ±0.10	2.02 ±0.02	1.21 ±0.08	50

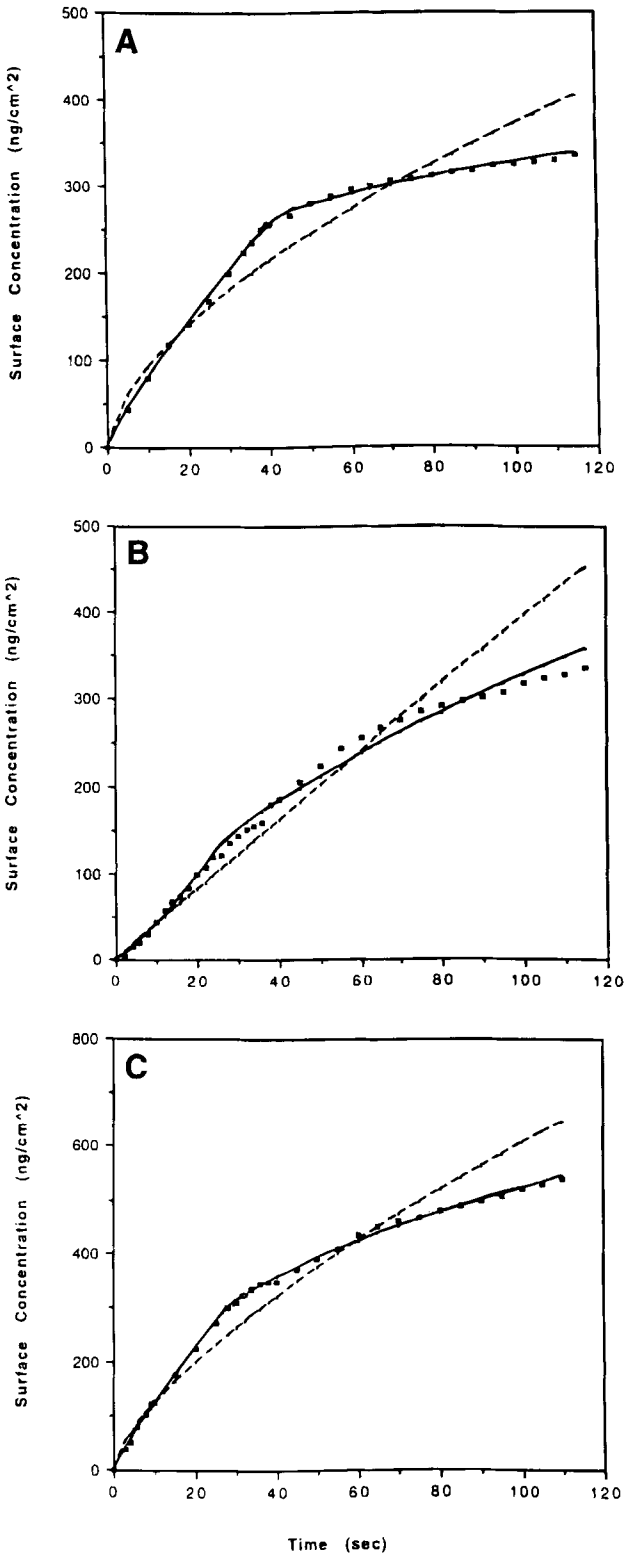

Fig. 2. Theoretical curves using Eqs. (3 and 4) for the binding of different monoclonal antibodies in solution to surface immobilized antigen (original data from Nygren, 1994): **(A)** MAb 49; **(B)** MAb 53; **(C)** MAb 57.

It is of interest to note the relative values of the binding rate coefficients (k, k_1, and k_2) and the fractal dimension (D_f, D_{f1}, and D_{f2}) as one compares the single-fractal analysis with a dual-fractal analysis. Note that $k_1 < k$ and $D_{f1} < D_f$. However, $k_2 > k$ and $D_{f2} > D_f$. The utilization of a dual-fractal analysis as compared to a single-fractal analysis leads initially to a decrease in both the binding rate coefficent, k_1 (compared to k) and in the fractal dimension, D_{f1} (compared to D_f). After time, $t = t_1$ the binding coefficient, k_2 and the fractal dimension, D_{f2} are both higher in value than k and D_f, respectively. It would be of interest to note if a similar decrease followed by an increase is obtained for antigen-antibody binding in other biosensor applications. Also, note that $D_{f2} > D_{f1}$. This indicates that as time increases, the fractal dimension or the state of disorder on the surface increases. This is to be intuitively expected. There is an 88.1% increase in the fractal dimension. Furthermore, $k_2 > k_1$. Thus, as time increases the binding rate coefficient also increases. An 88.1% increase in the fractal dimension leads to an increase in the binding rate coefficient by a factor of 4.48. This increase in the binding rate coefficient with an increase in the fractal dimension has been observed before for antigen-antibody binding in other biosensor applications *(22,23)*. These results were obtained on comparing the results of separate experiments. In the present case this holds for the same experiment.

Nygren *(43)* recently analyzed the binding of three different monoclonal antibodies, MAb 49, MAb 53, and MAb 57 to surface-immobilized antigen. Figs 2A–C show the curves obtained using Eq. (3 and 4) for the binding of MAb 49, MAb 53, and MAb 57, respectively to surface immobilized antigen. Table 1 shows the values of the binding rate coefficents and the fractal dimension values. Once again, clearly, the fit obtained by a dual-fractal analysis is better than that obtained by a single-fractal analysis. Also, as noted above in Fig. 1, for the binding of FITC-avidin in solution to sensor tips doped with 0.28 mol% DPPE *(42)* $k_1 < k$ and $D_{f1} < D_f$, and $k_2 > k$ and $D_{f2} > D_f$ for the binding of the different MAbs 49, 53, and 57 to surface immobilized antigen. Once again, the fractal dimension and the binding rate coefficient increase as the reaction (or the binding) progresses on the biosensor surface for all of the three monoclonal antibodies utilized. For example, for MAb 49, a 90.4% increase in the fractal dimension leads to an increase in the binding rate coefficient by a factor of 9.4.

In the examples to be presented henceforth, the dual-fractal analysis also clearly provides a better fit than a single fractal analysis. The values of the binding rate coefficients and the fractal dimension values obtained by both the single- and the dual-fractal analysis are given in Table 1. This permits a further comparision of the binding rate coefficient(s) and fractal dimension values for the two different analysis.

Dual-Fractal Analysis

Nygren *(43)* has recently analyzed the influence of monoclonal antibody MAb 53 concentration in solution on its binding to surface-immobi-

lized antigen. Figures 3A and B show the curves obtained using Eq. (3 and 4) for the binding of 30 and 100 μg/mL of MAb 53 to surface immobilized antigen. Table 1 shows the values of the binding rate coefficients and the fractal dimension values using a single- and dual-fractal analysis. Once again, as observed above, one notes that on comparing the single-fractal analysis with a dual-fractal analysis that $k_1 < k$ and $D_{f1} < D_f$, and $k_2 > k$ and $D_{f2} > D_f$ for the binding of the 30 and 100 μg/mL MAb 53 concentrations in solution to surface-immobilized antigen. It is of interest to note that an increase of MAb 53 concentration from 30 to 100 μg/mL leads to increases in the binding rate coefficient values for either the single-fractal *(k)* or the dual-fractal (k_1, k_2) analysis. Just for this case, as one increases the MAb 53 concentration in solution, one notes that the changes in the binding rate coefficient for the single-fractal analysis is more sensitive than that observed for the dual-fractal analysis. As one increases the MAb 53 concentration by a factor of 3.3 from 30 to 100 μg/mL, the *k* value changes by a factor of 4.15 from 6.57 to 27.3, the k_1 value changes by a factor of 1.84 from 4.94 to 9.09, and the k_2 value changes by a factor of 2.35 from 41.4 to 97.3. As indicated in the previous two examples, the fractal dimension and the binding rate coefficient both increase as the reaction progresses on the biosensor surface.

Mason and Williams *(44)* indicate that antibodies are finding increasing utilization for the identification, assay, and purification of membrane molecules. These authors indicate that indirect binding assays with ^{125}I-labeled anti-immunoglobulin can be utilized in several ways. Letarte-Muirhead et al. *(45,46)* have utilized binding assays to purify Thy-1 antigen (a membrane antigen). Indirect binding assays may also be utilized to analyze other complex antisera *(47–49)*. Mason and Williams *(44)* have recently analyzed the kinetics of association and dissociation of antibody interactions with cell-surface antigens in polymeric or monomeric forms. These authors utilized monoclonal antibodies since conventional antibodies are heterogeneous and are present in low concentrations in serum. Useful results from experiments performed on conventional antibodies are difficult to obtain.

Figure 4A shows the fit of the curve obtained using Eq. 3 and 4 for the binding of 25 μL of antibody and 25 μL of 0.5% deoxycholate incubated with 5×10^6 fixed rat thymocytes (50 μL in 5% BSA) in solution to cell-surface antigens. Table 1 shows the values of k, k_1, k_2, D_f, D_{f1}, and D_{f2}. This is clearly not a fiberoptic biosensor application. Nevertheless, an immunological reaction (antigen-antibody) takes place here, and the physical insights gained should be of assistance to understand immunological reactions on a fiberoptic biosensor surface. As indicated in the examples above, once again, $k_1 < k$ and $D_{f1} < D_f$, and $k_2 > k$ and $D_{f2} > D_f$. Similar results are obtained for the binding of 25 μL of antibody that was preincubated for 60 min with 25 μL of brain Thy-1 antigen (12.5 ng) in 0.5% deoxycholate (*see* Fig. 4B and Table 1). Also, the binding of 25 μL of ^{125}I-labeled rabbit F(ab')$_2$ anti-Thy-1 antibody in 0.5% deoxycholate in solution to cell-surface anti-

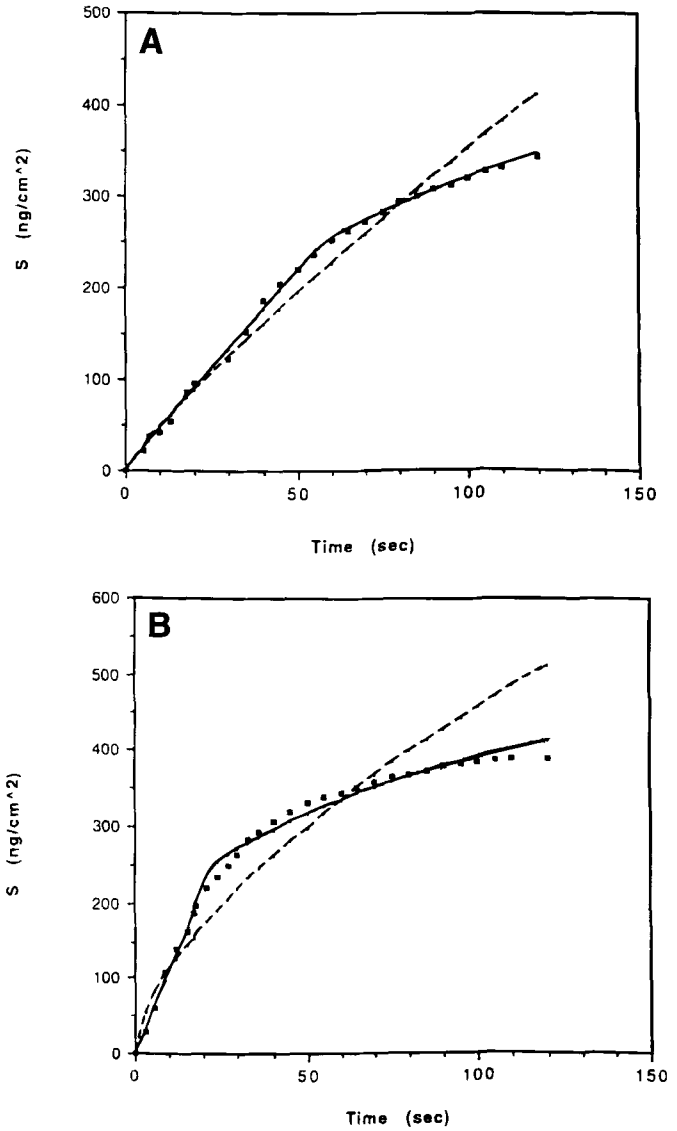

Fig. 3. Theoretical curves using Eqs. (3 and 4) for the binding of two different concentrations (μg/mL) of monoclonal antibody MAb 53 in solution to surface-immobilized antigen (original data from Nygren, 1994): **(A)** 30; **(B)** 100.

gens yields results similar to the ones exhibited above (*see* Fig. 4C and Table 1). Once again, one notes that both the fractal dimension (D_{f1} to D_{f2}) and the binding rate coefficient (k_1 to k_2) increase as the reaction or time progresses.

Fiberoptic chemical sensors were developed to detect a tetrol metabolite of BaP, r-7,t-8,9,c-10-tetrahydroxy-7,8,9,10-tetrahydrobenzo[a]pyrene (BPT)*(50)*. This was done in order to analyze the influence of regeneration on the biosensor performance. Figure 5 shows the binding rate curves

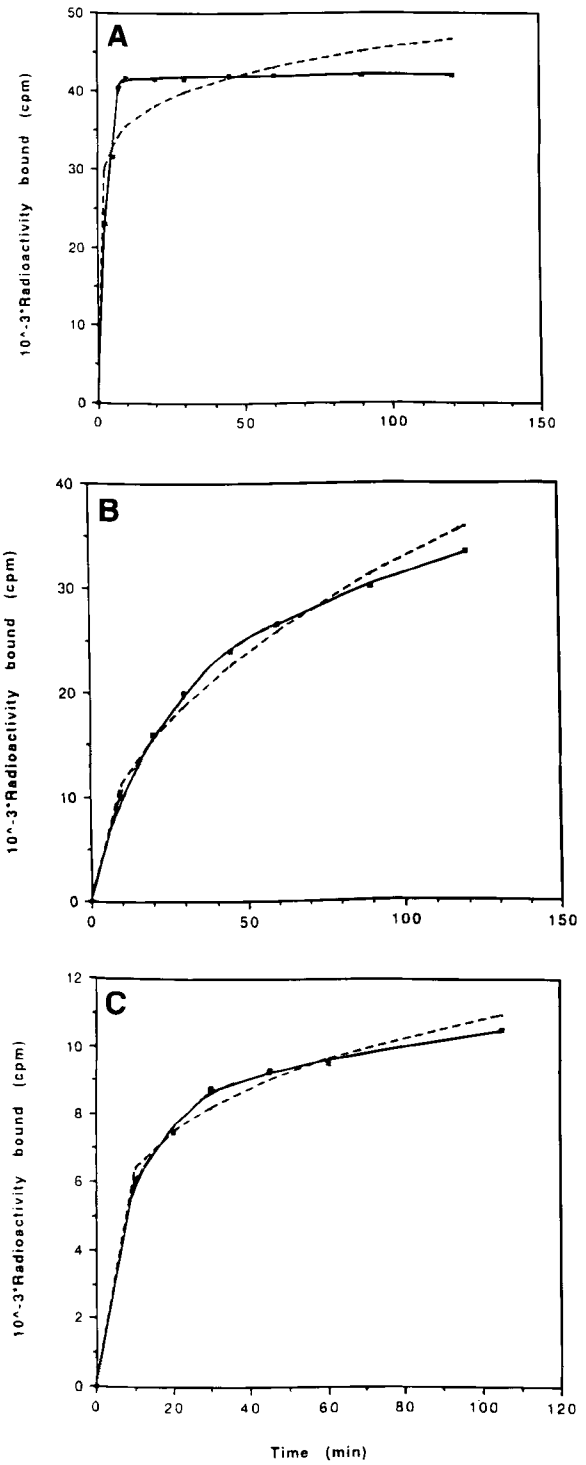

Fig. 4. Theoretical curves using eqs. (3 and 4) for the binding of antibody in solution to antigen from rat thymocyte (Thy-1.1) on the cell surface (original data from Mason and Williams, 1980): **(A)** 25 µL of antibody (12 ng; 5×10^4 cpm) and 25 µL of 0.5% deoxycholate; **(B)** 25 µL of antibody was preincubated for 60 min with 25 µL of brain Thy-1 antigen (12.5 ng) in 0.5% deoxycholate; **(C)** 25 µL of ^{125}I-labeled rabbit F(ab')$_2$ anti-Thy-1 antibody in 0.5% deoxycholate.

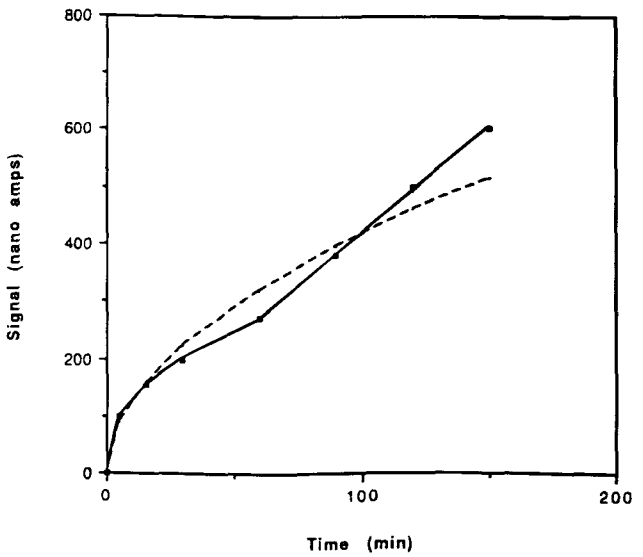

Fig. 5. Theoretical curves using Eqs. (3 and 4) for the binding of anti-rabbit IgG (BPT) in solution to rabbit IgG immobilized on an optical fiber (original data from Sepaniak et al., 1989).

obtained using Eqs. (3 and 4) for a fresh immunosensor. Table 1 shows the values of the fractal dimension(s) and the binding rate coefficient(s) using a single- as well as a dual-fractal analysis. In this case, one notes that there is a reversal in the trend in comparing the results with the previous examples. On comparing the single-fractal analysis with the dual-fractal analysis one notes that $k_1 > k$ and $D_{f1} > D_f$, and $k_2 < k$ and $D_{f2} < D_f$. Note that in this case as time increases both the fractal dimension and the binding rate coefficent decrease as the reaction progresses. No explanation is offered for this decrease in the fractal dimension as well as in the binding rate coefficient with time. Note that in this case a decrease in the fractal dimenson by 40.4% (D_{f1} to D_{f2}) decreases the binding rate coefficient by a factor of 7.74 (k_1 to k_2).

It is of interest to note that changes in the binding rate coefficient are in the same direction as that of the changes in the fractal dimension. This is an initial study. The analysis of data for the antigen-antibody binding for other biosensor applications is required to more firmly establish this change in the fractal dimension as well as the binding rate coefficient in the same direction during the same experiment.

CONCLUSIONS

The dual-fractal analysis of the binding of the antigen (or antibody) in solution to the antibody (or antigen) immobilized on the biosensor surface provides a quantitative indication of not only the state of disorder

and the binding rate coefficient on the surface, but also of the change in the state of disorder and the accompanying change in the binding rate coefficient. In some cases, the dual-fractal analysis provides an improved fit when compared to a single-fractal analysis. This was indicated by the regression analysis [sum of the $(\text{error})^2$] provided by Sigmaplot. The error being the difference between the theoretical predicted value and the experimental value. This was further corroborated by visual inspection of the figures presented for fitting the data by a single- and a dual-fractal analysis. During the same experiment, changes in the fractal dimension (D_{f1} to D_{f2}) are in the same direction as that of the binding rate coefficient (k_1 to k_2). In general, the increase in the fractal dimension leads to an increase in the binding rate coefficient as the reaction progresses on the biosensor surface. Also, for the single example presented, the decrease in the fractal dimension leads to a decrease in the binding rate coefficient on the biosensor surface. There is direct *(27)* and indirect evidence *(15)* to suggest that an increasing "roughness" on the surface would tend to increase the adsorption or binding rate coefficient.

Further analysis is required of other antigen-antibody binding reactions on biosensor surfaces to further delineate the changes in the fractal dimension and in the binding rate coefficients in the same direction. This type of analysis provides physical insights into the antigen-antibody reactions occurring on the biosensor surface, and would lead to a better control of the biosensor performance parameters such as stability, selectivity, sensitivity, and response time.

REFERENCES

1. Pisarchick, M. L., Gesty, D. and Thompson, N. L. (1992), *Biophys. J.* **63**, 215–223.
2. McLean, M. A., Stayton, P. S., and Sligar, S. G. (1993), *Anal. Chem.* **65**, 2676–2678.
3. Maxia, L., Radicchi, G., Pepe, I. M., and Nicolini, C. (1995), *Biophys. J.* **69**, 1440–1446.
4. Dubrovsky, T., Tronin, A., Dubrovskaya, S., Vakula, S., and Nicolini, C. (1995), *Sensors Actuators* **B23**, 1–7.
5. Bluestein, B.I., Craig, M., Slovacek, R., Stundtner, L., Uricouli, C., Walziak, I., Luderer, A. (1991), in *Biosensors With Fiberoptics*, Wise, D. and Wingard, Jr., L.B., eds., Humana, Clifton, NJ, pp. 181–223.
6. Eddowes, E. (1987/1988), *Biosensors* **3**, 1–15.
7. Giaver, I. (1976), *J. Immunol.* **116**, 766–771.
8. Stenberg, M., Stiblert, L. and Nygren, H. A. (1986), External Diffusion Solid-Phase Immunoassay. *J. Theor. Biol.* **120**, 129–142.
9. Nygren, H. A. and Stenberg, M. (1985), *J. Colloid Interf. Sci.* **107**, 560–566.
10. Stenberg, M. and Nygren, H. A. (1982), *Anal. Biochem.* **127**, 183–192.
11. Sadana, A. and Sii, D. (1992), *Biosens. Bioelectron.* **7**, 559–568.
12. Sadana, A. and Sii, D. (1992), *J. Colloid Interf. Sci.* **151**, 166–177.
13. Sadana, A. and Madagula, A. (1993), *Biotechnol. Progr.* **9**, 259–266.
14. Sadana, A., Alarie, J. P. and Vo-Dinh, T. (1995), *Talanta* **42**, 1567–1574.
15. Douglas, J. F. (1989), *Macromolecules* **22**, 3707–3716.
16. Ortega-Vinuesa, J. L., Bastos-Gonzalez, D. and Hidalgo-Alvarez, R. (1995), *J. Colloid Interf. Sci.* **176**, 240–247.

17. Kopelman, R. (1988), *Science* **241**, 1620–1626.
18. Metzler, R., Glockle, W. G., and Nonnenmacher, T. F. (1994), *Physica A* **211**, 13–24.
19. Giona, M. and Roman, H. E. (1992), *Physica A* **185**, 87–97.
20. Werthen, M. and Nygren, H. A. (1993), *Biochim. Biophys. Acta* **1162**, 326–332.
21. Pfeifer, P. and Obert, M. (1989), in *The Fractal Approach To Heterogeneous Chemistry: Surfaces, Colloids, Polymers*; Avnir, D., ed., J. Wiley & Sons, New York, NY, pp. 11–43.
22. Sadana, A. and Beelaram, A. (1994), *Biotechnol. Progr.* **10**, 291–298.
23. Sadana, A. and Beelaram, A. (1995), *Biosens. Bioelectron.* **10**, 301–316.
24. Sadana, A. and Beelaram, A. (1996), *Appl. Biochem. Biotechnol.* **60**, 123.
25. Sadana, A. and Beelaram, A. (1997), *Appl. Biochem. Biotechnol.* (in press).
26. Sadana, A. and Madagula. A. (1994), *Biosens. Bioelectron.* **9**, 45–55.
27. Sadana, A. (1995), *Biotechnol. Progr.* **11**, 50–57.
28. Skinner, J. E. (1994), *Bio/Technology* **12**, 596–600.
29. Cross, M. C. and Hohenberg, P. C. (1994), *Science* **263**, 1569–1570.
30. Vlad, M. O. (1993), *J. Colloid Interf. Sci.* **159**, 21–27.
31. Friesen, W. I. and Laidlaw, W. G. (1993), *J. Colloid Interf. Sci.* **160**, 226–235.
32. Glockle, W. G. and Nonnenmacher, T. F. (1995), *Biophys. J.* **68**, 46–53.
33. Shlesinger, M. F., Zaslavsky, G. M., and Klafter, J. (1993), *Nature* **363**, 31–37.
34. Rabinovich, S, and Agmon, N. (1993), *Phys. Rev. E* **47**, 3717–3720.
35. Di Cera, E. (1991), *J. Chem. Phys.* **95**, 5082–5086.
36. Cuypers, P. A., Willems, G. M., Kop, J. M., Corsel, J. W., Jansen, M. P., and Hermens, W. T. (1987), in *Proteins At Interfaces. Physicochemical And Biochemical Studies*. Brash, J. L., Horbett and T.A., eds., American Chemical Society, Washington, DC, pp. 208–211.
37. Anderson, J., (1993), NIH Panel Review Meeting, Case Western Reserve University, Cleveland, OH.
38. De Gennes, P. G. (1982), *Radiat. Phys. Chem.* **22**, 193–196.
39. Pfeifer, P., Avnir, D. and Farrin, D. J. (1984a), *Nature* **308**, 261–263.
40. Pfeifer, P., Avnir, D. and Farin, D. J. (1984b), *J. Colloid Interf. Sci.* **103**, 112–123.
41. Nyikos, L. and Pajkossy, T. (1986), *Electrochim. Acta* **31**, 1347–1350.
42. Havlin, S. (1989), in *The Fractal Approach To Heterogeneous Chemistry: Surfaces, Colloids, Polymers*; Avnir, D., ed., J. Wiley & Sons, New York, NY, pp. 251–269.
42. Zhao, S. and Reichert, W. M. (1992), *Langmuir* **8**, 2785–2791.
43. Nygren, H. A. (1994), *Biophys. Chem.* **52**, 45–50.
44. Mason, D. W. and Williams, A. F. (1980), *Biochem. J.* **187**, 1–20.
45. Letarte-Muirhead, M., Acton, R. T., and Williams, A. F. (1974), *Biochem. J.* **143**, 51–61.
46. Letarte-Muirhead, M., Barclay, A.N. and Williams, A.F. (1975), *Biochem. J.* **151**, 685–697.
47. Fabre, J. W. and Williams, A. F. (1997), *Transplantation* **23**, 349–359.
48. MacDonald, M. E., Letarte-Muirhead, M., and Bernstein, A. (1978), *J. Cell Physiol.* **96**, 291–302.
49. Dalchau, R. and Fabre, J. W. (1979), *J. Exp. Med.* **149**, 576–591.
50. Sepaniak, M. J., Tromberg, B. J., and Estham, J. F. (1983), *Chin, Chem.* **29**, 1678.